Available online at www.sciencedirect.com
ScienceDirect
Solar Energy 85 (2011) 1574–1578
SOLAR ENERGY
www.elsevier.com/locate/solener

Brief Note

A novel method to produce black silicon for solar cells

Yang Xia *, Bangwu Liu *, Jie Liu, Zenan Shen, Chaobo Li

Key Laboratory of Microelectronics Devices & Integrated Technology, Institute of Microelectronics, Chinese Academy of Sciences, Beijing, China

Received 13 December 2010; received in revised form 11 March 2011; accepted 14 March 2011
Available online 22 April 2011

Communicated by: Associate Editor Dr. Takhir Razykov

Abstract

In the present study, the black silicon has been successfully produced by plasma immersion ion implantation (PIII). The microstructure and the reflectance of the black silicon have been investigated by field emission scanning electron microscope and spectrophotometer, respectively. Results show that the black silicon exhibits a needle-like structure with the average reflectance of 1.79%. The solar cell based on black silicon yields an efficiency of 15.68% with a fill factor (FF) of 0.783.

Keywords: Black silicon; Solar cell; Microstructure; Reflectance; Conversion efficiency

1. Introduction

To reduce the front surface reflectance of crystalline silicon solar cells is one of the most important points to improve the cells efficiency. Various kinds of ways of texturing silicon surfaces have been used to reduce the reflectance. For example, anisotropic etching of single-crystalline in alkaline solution can form random pyramids, which has been widely used in industry. In the case of multi-crystalline Si (mc-Si) this method is not effective because there are few (1 0 0) oriented grains on mc-Si wafer (Panek et al., 2005). The acid texturing approach is instrumental to achieve high efficiency in mass production using relatively low-cost mc-Si as starting material with proper optimization of the fabrication steps (Cheng et al., 2011). Mechanical structuring of silicon surfaces is a more efficient method, but it is not cheap enough for solar cells at industrial level (Gerhards et al., 1997). Another method to reduce the reflectance is to etch the silicon surface using reactive ion etching (RIE). Yoo (2010) have obtained texturing single crystalline silicon with sparsely distributed crater-like pyramidal structures by RIE, which shows 8.9% optical reflectance in the wavelength range of 300–850 nm. Macdonald et al. (2004) have obtained texturing industrial multicrystalline silicon for solar cells with an optical reflectance of 11% by markless RIE. However, RIE will cause the ion damage and it is a complex and expensive process, which limits its application to produce low cost high efficiency solar cells (Moreno et al., 2010; Zaidi et al., 2001). Recently, irradiating the silicon surface with a series of femtosecond laser pulses in SF_6 has been reported (Her et al., 1998; Younkin et al., 2003; Crouch et al., 2004). Although the reflectance can be reduced greatly by this method, it is also very expensive and too slow to adapt the high throughput industrial applications.

Plasma immersion ion implantation (PIII) is usually used to dope semiconductors. The physical principle of plasma immersion ion implantation is illustrated elsewhere (Cheung, 1996). In the present study, the "black silicon" with very low reflectance has been produced by plasma immersion ion implantation (PIII). The microstructure and the reflectance of the black silicon will be investigated. The solar cell based on black silicon has been fabricated. And the performance of the black silicon solar cells will be studied.

* Corresponding authors. Tel.: +86 10 82995526; fax: +86 10 82995652 (Y. Xia), tel.: +86 10 82995758; fax: +86 10 82995652 (B. Liu).
E-mail addresses: xiayang@ime.ac.cn (Y. Xia), liubangwulbw@163.com (B. Liu).

0038-092X/$ - see front matter © 2011 Elsevier Ltd. All rights reserved.
doi:10.1016/j.solener.2011.03.012

2. Experimental

The material used for experiments was commercially available boron doped p-type single-crystalline silicon wafers obtained from the ingot by wire sawing of thickness ~190 μm, area 125 mm × 125 mm and resistivity 1–3 Ω cm. Damage on the surface induced by wire-cutting was removed by etching in 10% NaOH solution at 80 °C. The black silicon was prepared by plasma immersion ion implantation process on home-made equipment. O_2 and SF_6 gas was bled into the vacuum chamber at a flow rate of 20 and 90 sccm, respectively. The working pressure was 0.86 Pa. 900 W radio frequency power was matched to the plasma discharge chamber to generate the plasma. −500 V negative voltage pulses were applied to the sample stage during the PIII process. During the PIII process, SF_6 and O_2 will be ionized reactive ions and radicals. Under the negative voltage, the reactive ions are injected into the silicon substrate and react with silicon. The pulse duration was 30 μs and the total treatment time was 10 min.

After the PIII treatment, the wafers were subjected to acid etching in 2% HCl and then in 10% HF to remove the contamination and oxides. Then, the wafers were phosphorus doped using with phosphorous oxychloride ($POCl_3$) as the dopant source at a diffusion temperature of 868 °C. On removal of phosphosilicate glass (PSG) layer from the diffused wafers surface with diluted HF (10% by volume), the wafers were subjected to edge etching. Then silicon nitride (Si_3N_4) layer for passivation was grown by plasma enhanced chemical vapor deposition process. Then the back electrode was fabricated by screen printing using Ag–Al paste, Al paste and front side using Ag paste followed by baking and co-firing at a proper temperature. The complete process flow chart was shown in Fig. 1. The reference solar cell was also fabricated on textured silicon with pyramid structure which was obtained by wet etching in NaOH/IPA. The fabrication process of reference solar cell was identical with that of black silicon solar cell.

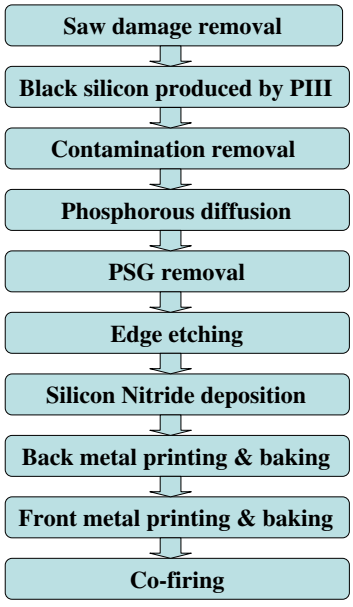

Fig. 1. Process flow chart of black silicon solar cell fabrication process.

The microstructure of the black silicon was investigated with JEOL JSM-7001F field emission scanning electron microscope (FESEM). The black silicon surface reflection was examined by a UV–VIS–NIR spectrophotometer (Cary-5000) equipped with an integrating sphere detector. External quantum efficiency (EQE) was performed on a Solar Cell Scan100 quantum efficiency measurement system. The defects in solar cell were detected by electroluminescence equipment.

3. Results and discussion

Fig. 2 shows the SEM images of unique microstructures of the black silicon. The black silicon surface exhibits a needle-like structure. The average height of the needle is about 2 μm. The formation mechanism of the needle-like structure produced by PIII process can be depicted in Fig. 3. During the PIII process, SF_6 plasma is composed of F^+, SF^+, SF_3^+, SF_5^+ ions and so on (Tessier et al., 1999). With addition of O_2, the plasma is also composed of the O^* radicals. Under the negative voltage, the SF_x^+ ($x \leqslant 5$) and F^+ ions are injected into the silicon substrate. Then these reactive ions will react with silicon to form volatile SiF_4 which escapes from the substrate. Consequently, the Si surface will be etched uniformly by SF_6 PIII process.

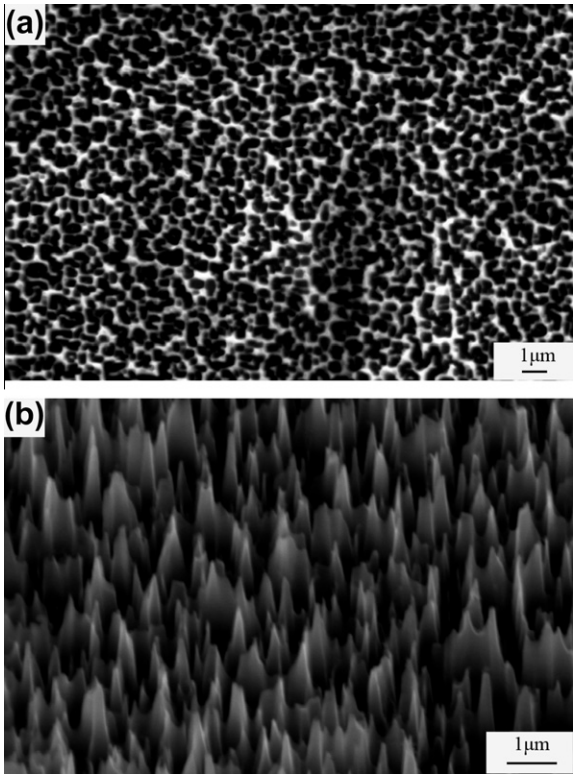

Fig. 2. SEM images of unique microstructures of the black silicon. (a) Top view, (b) side view (viewed at 30 ° to the normal).

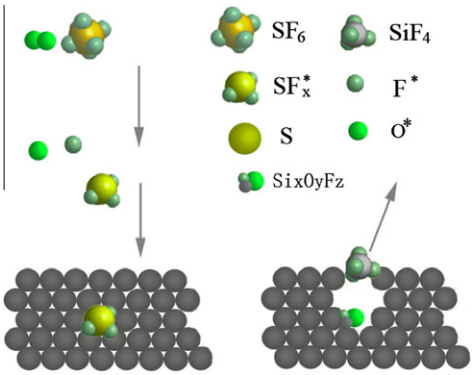

Fig. 3. The formation mechanism of needle-like structure by PIII process.

With the addition of O_2, O^*radicals will react with the fresh silicon surface rapidly to form SiO_x. The SiO_x will react with SF_x^+ ($x \leqslant 5$) and F^+ ions to form $Si_xO_yF_z$ because the binding energy of a Si–F bond (129.3 kcal/mol) is larger than that of Si–O (88.2 kcal/mol). Under the effect of ion bombardment, some $Si_xO_yF_z$ will escape from the silicon surface which will be etched by SF_x^+ ($x \leqslant 5$) and F^+ ions consequently. The porous or needle like structure of the black silicon will be formed under the competition of SF_x^+ ($x \leqslant 5$) and F^+ ions etching effect, $Si_xO_yF_z$ passivation and ion bombardment.

The reflectance of polished, textured and black silicon was measured over the wavelength ranging from 300 nm to 1100 nm (Fig. 4). The average reflectance (R_a) can be defined as (Menna et al., 1995):

$$R_a = \frac{\int_{300}^{1100} R(\lambda)N(\lambda)d\lambda}{\int_{300}^{1100} N(\lambda)d\lambda}$$

where $R(\lambda)$ – total reflectance, $N(\lambda)$ – the solar flux under AM1.5 standard conditions. The black silicon results in significant decrease in the value of the average reflectance compared to the polished and textured silicon. By calculation, the average reflectance of polished, textured and black silicon is 30.01%, 12.07% and 1.79%, respectively. The decreased reflectance of the black silicon is a result of the unique structure. The unique microstructure leads to multiple reflections for incoming light.

The electrical parameters of the reference and black silicon cell are listed in Table 1. In comparison with the reference cell, the black silicon cell has a larger series resistance and a smaller shunt resistance. This can be attributed to poor contact between electrode and wafer. With fill factor (FF) value of 0.783, the black silicon cell yields an efficiency of 15.68%.

Fig. 5 shows the external quantum efficiency (EQE) of the reference and black silicon solar cells. The EQE data of black silicon cell is lower than that of reference cell, especially at short wavelengths. Because high-energy (short wavelengths) light is absorbed very close to the surface, considerable recombination at the front surface will affect the EQE at short wavelengths. The EQE at short wavelengths is related with the response of the front surface of the cell. Therefore, the EQE of black silicon solar cell is reduced at short wavelengths due to surface recombination and additional recombination at the enormous internal surface. The surface recombination is closely related with doping concentration of P element. The doping concentration can be characterized by sheet resistance. The high doping concentration will lead to low sheet resistance. The sheet resistance of black silicon is ~33 Ω/□, much lower than that of the reference cell (~50 Ω/□), indicating

Table 1
Comparison of the electrical parameters of the reference and black silicon cells from the illuminated current–voltage (LIV) characteristics.

Cell parameters	Reference cell	Black silicon cell
Open circuit voltage (V)	0.621	0.619
Short circuit current density (mA/cm^2)	36	32
Efficiency (%)	17.5	15.68
Fill factor	0.78	0.783
Maximum power output (W)	2.59	2.33
Series resistance (mΩ)	6.67	8.5
Shunt resistance (Ω)	24.86	9.34

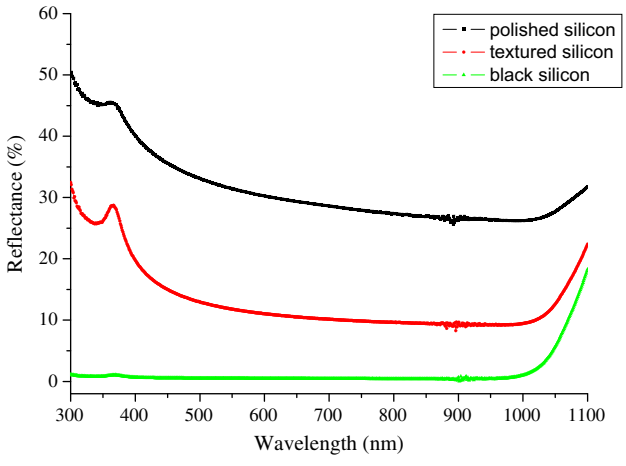

Fig. 4. The reflectance of polished, textured and black silicon.

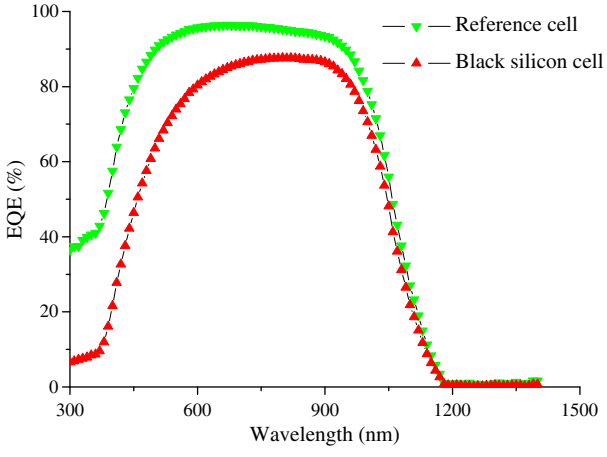

Fig. 5. The external quantum efficiency of the reference and black silicon cells.

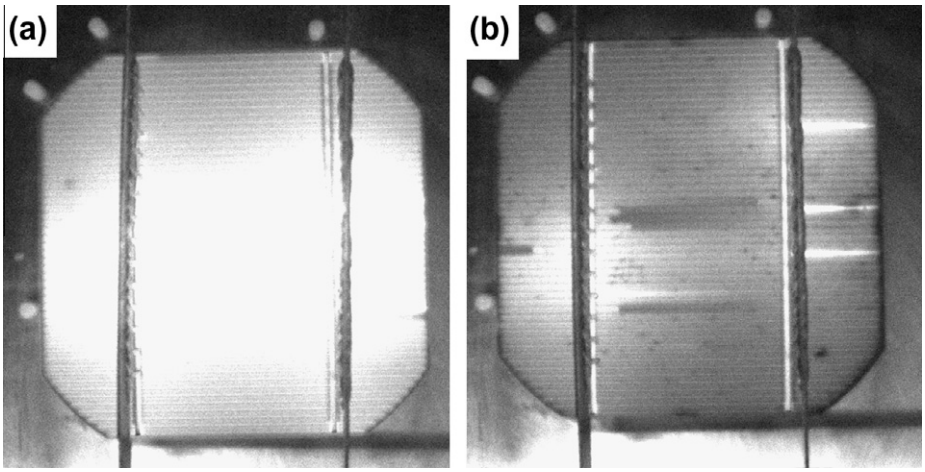

Fig. 6. The EL images of the reference and black silicon cell. (a) The reference cell, (b) the black silicon cell.

that the black silicon has a higher doping concentration. The reason is that P diffusion is easier in needle-like structure than pyramid structure under the same condition. Yuan et al. have also obtained that the quantum efficiency of the porous black silicon cell reduces below ~700 nm wavelength (Yuan et al., 2009). They explained that reduction of quantum efficiency results from the nanoporous "dead layers" due to a heavily doped Si (10^{21} cm^{-3} of P) with high Auger recombination.

The electroluminescence (EL) is the inverse effect of photovoltaic effect, where light emission caused by electrical current flow through a semiconductor with a pn junction (Yeh et al., 2008). The junction leakage area and the poor EL area represent the poor conversion efficiency locations of the solar cell (Fuyuki, 2006). Distribution and intensity of EL signals reflect solar cell conversion efficiency. Brighter and warmer color indicates places with higher solar cell conversion efficiency, while darker and colder color indicates places with lower conversion efficiency. Fig. 6 shows the EL image of the reference and black silicon cell. The EL intensity of black silicon cell is darker and colder than that of reference cell. The EL image indicates that the conversion efficiency of black silicon cell is lower than that of reference cell. The lower conversion efficiency of black silicon cell results from a high doping concentration. In Fig. 6b, it can be seen that there exist some dark area, indicating that the charge carrier may not be collected by the front electrode. This can be attributed to defect which interrupts the grid fingers in the front electrode (Fig. 7). Qi et al. (2009) have reported the black silicon exhibited superhydrophobic properties, leading to defect in the front electrode during screen printing process. And the defect will result in a low quality of the metallic contact placed on the black silicon surface compared to the reference cell.

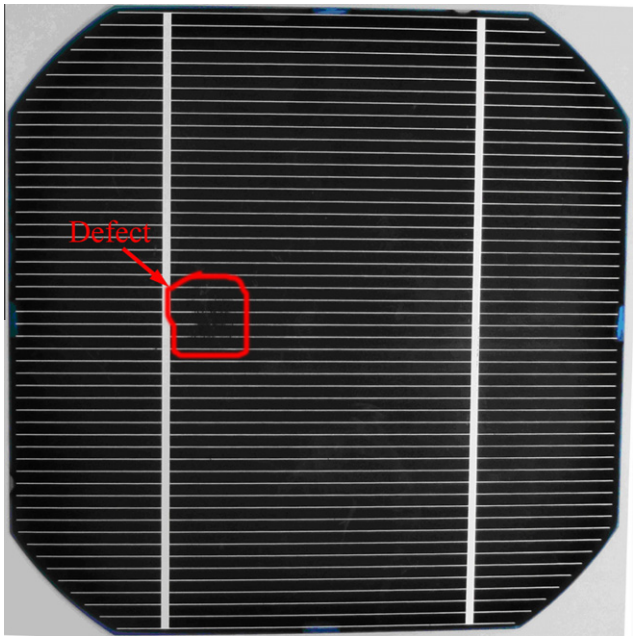

Fig. 7. The defect in the front electrode of black silicon cell.

4. Conclusions

The black silicon has been successfully produced by plasma immersion ion implantation (PIII). The black silicon exhibits a unique microstructure with a needle-like structure. The average reflectance of the black silicon can be reduced to 1.79% over the wavelength ranging from 300 nm to 1100 nm. The solar cell based on black silicon yields an efficiency of 15.68% with a fill factor value of 0.783. The conversion efficiency and quantum efficiency of the black silicon solar cell is lower than that of conventional cell, which results from a high doping concentration. The conversion efficiency of the black silicon solar cell may be further improved by optimize the phosphorous diffusion process and the front electrode process.

Acknowledgment

This work was supported by the National Natural Science Foundation of China (No. 607227003) and the Instru-

ment Developing Project of the Chinese Academy Sciences (No. YZ200755).

References

Cheng, Y.-T., Ho, J.-J., Tsai, S.-Y., et al., 2011. Efficiency improved by acid texturization for multi-crystalline silicon solar cells. Sol. Energy 85, 87–94.

Cheung, N.W., 1996. Plasma immersion ion implantation for semiconductor processing. Mater. Chem. Phys. 46, 132–139.

Crouch, C.H., Carey, J.E., Warrender, J.M., et al., 2004. Comparison of structure and properties of femtosecond and nanosecond laser-structured silicon. Appl. Phys. Lett. 84, 1850–1852.

Fuyuki, T., 2006. "Luminoscopy" A Versatile Tool for the Diagnosis of Crystalline Silicon Solar Cells Utilizing Electroluminescence. NAIST, POLYSE.

Gerhards, C., Marckmann, C., Tolle, R., et al., 1997. Mechanically V-textured low cost multicrystalline silicon solar cells with a novel printing metallization. In: Proceedings of the 26th IEEE Photovoltaic Specialists Conference, PVSC'97, Anaheim, pp. 43–46.

Her, T.H., Finlay, R.J., Wu, C., et al., 1998. Microstructuring of silicon with femtosecond laser pulses. Appl. Phys. Lett. 73, 1673–1675.

Macdonald, D.H., Cuevas, A., Kerr, M.J., et al., 2004. Texturing industrial multicrystalline silicon solar cells. Sol. Energy 76, 277–283.

Menna, P., Di Francia, G., La Ferrara, V., 1995. Porous silicon in solar cells, A review and description of its application as an AR coating. Sol. Energy Mater. Sol. Cells 37, 13–24.

Moreno, M., Daineka, D., Rocai Cabarrocas, P., 2010. Plasma texturing for silicon solar cells: from pyramid to inverted pyramid-like structures. Sol. Energy Mater. Sol. Cells 94, 733–737.

Panek, P., Lipinski, M., Dutkiewicz, J., 2005. Texturization of multicrystalline silicon by wet chemical etching for silicon solar cells. J. Mater. Sci. 40, 1459–1463.

Qi, D., Lu, N., Xu, H., et al., 2009. Simple approach to wafer-scale self-cleaning antireflective silicon surfaces. Langmuir 25, 7769–7772.

Tessier, P.Y., Chevolleau, T., Cardinaud, C., et al., 1999. An XPS study of the SF_6 reactive ion beam etching of silicon at low temperatures. Nucl. Instr. Meth. Phys. Res. B 155, 280–288.

Yeh, B., Huang, R., Chung, K., et al., 2008. EMMI Analysis on Silicon Solar Cell, Physical and Failure Analysis of Integrated Circuits

Yoo, J.S., 2010. Reactive ion etching (RIE) technique for application in crystalline silicon solar cells. Sol. Energy 84, 730–734.

Younkin, R., Carey, J.E., Mazur, E., et al., 2003. Infrared absorption by conical silicon microstructures made in a variety of background gases using femtosecond-laser pulses. J. Appl. Phys. 93, 2626–2629.

Yuan, H.-C., Yost, V.E., Page, M.R., et al., 2009. Efficient black silicon solar cell with a density-graded nanoporous surface: optical properties, performance limitations, and design rules. Appl. Phys. Lett. 95, 23501.

Zaidi, S.H., Ruby, D.S., Gee, J.M., 2001. Characterization of random reactive ion etched-textured silicon solar cells. IEEE Trans. Electron Devices 48, 1200–1206.